Resting State Correlates of Subdimensions of Anxious Affect

Janine Bijsterbosch[1,2], **Stephen Smith**[1], **Sophie Forster**[2], **Oliver P. John**[2], and **Sonia J. Bishop**[1,2]

[1]University of Oxford

[2]University of California-Berkeley

Abstract

Resting state fMRI may help identify markers of risk for affective disorder. Given the comorbidity of anxiety and depressive disorders and the heterogeneity of these disorders as defined by DSM, an important challenge is to identify alterations in resting state brain connectivity uniquely associated with distinct profiles of negative affect. The current study aimed to address this by identifying differences in brain connectivity specifically linked to cognitive and physiological profiles of anxiety, controlling for depressed affect. We adopted a two-stage multivariate approach. Hierarchical clustering was used to independently identify dimensions of negative affective style and resting state brain networks. Combining the clustering results, we examined individual differences in resting state connectivity uniquely associated with subdimensions of anxious affect, controlling for depressed affect. Physiological and cognitive subdimensions of anxious affect were identified. Physiological anxiety was associated with widespread alterations in insula connectivity, including decreased connectivity between insula subregions and between the insula and other medial frontal and subcortical networks. This is consistent with the insula facilitating communication between medial frontal and subcortical regions to enable control of physiological affective states. Meanwhile, increased connectivity within a frontoparietal–posterior cingulate cortex–precunous network was specifically associated with cognitive anxiety, potentially reflecting increased spontaneous negative cognition (e.g., worry). These findings suggest that physiological and cognitive anxiety comprise subdimensions of anxiety-related affect and reveal associated alterations in brain connectivity.

INTRODUCTION

It has been suggested that resting state fMRI may be used to obtain biomarkers of disease state (Cole, Smith, & Beckmann, 2010). Recently, there has been increasing recognition within the psychiatric community that, given the heterogeneity of many disorders, attempts to map neural or genetic biomarkers directly onto DSM-defined diagnostic status may be of limited value in advancing our understanding of the mechanisms involved in risk for and etiology of disease state.

In the case of anxiety disorders, an additional challenge arises from the extent of common variance and indeed shared heritability between anxiety and depressive disorders (Hettema et al., 2008; Kendler, Gardner, Gatz, & Pedersen, 2007; Costa & McCrae, 1995; Clark & Watson, 1991). It is probable that some alterations in resting state brain connectivity will be unique to anxiety whereas others will be shared with depression. Given the heterogenous

symptomatology of anxiety disorders, it also seems likely that distinct alterations in regional brain function or connectivity will underlie different dimensions of anxiety-related affect.

In meeting this challenge, we are helped by the availability of a number of standardized continuous self-report measures of negative affect. These derive from both the clinical and personality literatures and span cognitive and physiological aspects of anxious affect, depressed affect, and neurotic personality style. Within the neuroimaging literature, there has been a tendency to use one of these measures at a time. This makes it difficult to reconcile findings between studies and to determine whether identified alterations in resting brain connectivity are specific to anxiety versus depression or indeed associated with a particular profile of anxiety-related affect.

In the 1990s, recognition of the need to distinguish anxious and depressed affect led to the development of the Mood and Anxiety Symptom Questionnaire (MASQ; Watson & Clark, 1991). This measure has not previously been used to differentiate resting state connectivity correlates of anxious versus depressed affect. It may be valuable for differentiating physiological symptoms of anxiety from symptoms of anhedonia linked to depression. However, the MASQ does not provide optimal coverage of cognitive aspects of anxiety (e.g., worry) or of the presence of negative mood in depression (as opposed to absence of positive affect). Other standardized measures that do provide this coverage are available (Meyer, Miller, Metzger, & Borkovec, 1990; Radloff, 1977; Beck, Ward, Mendelson, Mock, & Erbaugh, 1961). Through combined use of these measures, it may be possible to advance our understanding of alterations in resting state brain function that are unique to anxiety as opposed to depression.

Above, we have focused on the potential value in going beyond DSM diagnostic categories and single self-report measures in investigating anxiety-related alterations in resting state functional brain connectivity. Another important issue pertains to the choice of resting state fMRI analysis for probing individual differences in brain connectivity. In the literature to date, seed-based approaches have been most common, whereas a smaller number of studies have used data-driven approaches such as independent component analysis (ICA).

Seed-based analyses of altered resting state functional connectivity in anxiety have primarily focused on patterns of amygdala connectivity. These studies have revealed reduced connectivity between the amygdala and both the medial OFC and the middle temporal gyrus in patients with social phobia (Pannekoek et al., 2012; Hahn et al., 2011). Meanwhile, decreased connectivity between the amygdala and both the insula and ACC has been reported in generalized anxiety disorder (Etkin, Prater, Schatzberg, Menon, & Greicius, 2009). In contrast, elevated trait anxiety, as measured by the Spielberger State–Trait Anxiety Inventory (STAI), has been linked to increased amygdala–insula connectivity (Baur, Hänggi, Langer, & Lutz, 2012). In addition, both high STAI state and trait anxiety have been associated with altered balance of connectivity between the amygdala and ventral versus dorsal medial pFC (Kim, Gee, Loucks, Davis, & Whalen, 2011). A further study using Neuroticism as the measure of interest and precuneous as the seed region reported increased connectivity between the precuneous and dorsomedial pFC (Adelstein et al., 2011).

Adopting a contrasting data-driven approach, two studies have used ICA to examine brain networks modulated by global state anxiety (measured using a single self-report item). One study reported that high global state anxiety was linked to increased connectivity within a "salience" network including the dorsal anterior cingulate, amygdala, and insula (Seeley et al., 2007). Another showed increased connectivity between the left insula and the default mode network (Dennis, Gotlib, Thompson, & Thomason, 2011).

In the current work, we seek to combine the advantages of the hypothesis-driven approach afforded by seed-based analyses, with the greater data-driven flexibility and breadth that characterizes dimension reduction approaches such as ICA. One potential hybrid approach involves the application of multivariate clustering analysis to a relatively large number of a priori ROIs previously implicated in the domain under consideration. Here, we apply a hierarchical clustering approach in parallel to both resting state fMRI data and to participants' scores on multiple standardized self-report measures of negative affect. This two-phase multivariate approach enables us to identify alterations in resting state functional connectivity uniquely linked to dimensions of anxious as opposed to depressed affect. Previous work has adopted a conceptually comparable multivariate approach (partial least squares) to explain the relationship between regional brain activity or volumetric measures and task performance (McIntosh, Chau, & Protzner, 2004; McIntosh, Bookstein, Haxby, & Grady, 1996).

The aim of this work is to determine if resting state connectivity correlates uniquely associated with anxiety, independent of depressed affect. We adopted a two-phase approach to maximize power for our multivariate analyses. In the first phase, over 300 participants completed a battery of standardized self-report measures of negative affect online. Hierarchical clustering analysis of these data enabled us to identify four subdimensions of negative affect: two anxiety-related and two depression-related. Subsequently, we applied a parallel hierarchical clustering analysis to resting state data collected from a novel sample of 19 participants who also completed the same battery of self-report measures. Bringing the self-report and imaging results together revealed individual differences in brain connectivity patterns uniquely linked to each of the emergent subdimensions of anxiety, independent of variance associated with depressed affect.

METHODS

Participants

In Phase 1, 379 participants filled out a battery of self-report measures of negative affect online. Complete data were obtained from 327 participants (203 women; mean age = 21.1 years). In Phase 2, 19 participants (14 women, all right-handed, aged 18–28 years, mean age = 21.5 years) took part in a resting state study while fMRI data were acquired. In Phase 2, participants were selectively recruited to show a wide range of scores on anxiety-related measures using a local database of potential participants who had been screened for inclusion (e.g., age range) and exclusion (e.g., metal implant free) criteria and administered a range of self-report measures. This maximized statistical power for the investigation of anxiety-related dimensions of negative affect. This study was approved by the University of California-Berkeley Committee for the Protection of Human Subjects and carried out in compliance with their guidelines. Written informed consent was obtained from participants before participation. Individuals with a history of psychiatric care, neurological disease or head injury, or taking psychotropic medication, were excluded.

Questionnaire Measures of Negative Affect

Participants completed nine standardized measures of negative affect. These were chosen to broadly cover the domain of negative affect as assessed in the anxiety, depression, and personality literatures and to encompass both cognitive and physiological or somatic features. Trait anxiety was measured using the Spielberger STAI, form Y (Spielberger, 1983). The STAI trait subscale is the main standardized trait measure of anxiety available and widely used in the affective cognitive neuroscience literature. Scores on the STAI trait subscale are elevated in individuals meeting criteria for anxiety disorders across subtypes (Chambers, Power, & Durham, 2004; Bieling, Antony, & Swinson, 1998) and predict future

anxiety disorder diagnosis (Plehn & Peterson, 2002). However, STAI trait anxiety scores are also elevated in individuals with major depressive disorder (Chambers et al., 2004). It has been argued that the STAI trait subscale can be broken down into two clusters of items: one tapping trait anxiety and one tapping trait depression (Bieling et al., 1998). These two subclusterings of items were used here. Consideration of item content reveals that the "depression" items are best described as "anhedonic" items as they pertain to the absence of positive mood or normal enjoyment of life and everyday activities.

We also administered the MASQ (Watson & Clark, 1991). This includes subscales for anxious arousal and anhedonic depression. The anxious arousal subscale addresses physiological/somatic aspects of anxiety. To obtain a measure of cognitive aspects of anxiety, we included a commonly used measure of worry, the Penn State Worry Questionnaire (Meyer et al., 1990). As a final measure on the anxiety side, fear of anxiety-related symptoms was measured using the Anxiety Sensitivity Index (Reiss, Peterson, Gursky, & McNally, 1986). On the depression side, we added in the Beck Depression Inventory (Beck et al., 1961) and the Center for Epidemiologic Studies Depression Scale (Radloff, 1977). These are the two most commonly used measures of depressive affect and provide coverage of the negative mood aspects of depression. From the personality literature, we administered the 48-item short-scale version of the Eysenck Personality Questionnaire (Eysenck, Eysenck, & Barrett, 1985; Eysenck & Eysenck, 1975). The Eysenck Personality Questionnaire includes one measure relevant to negative affect, namely the 12-item Neuroticism scale, which we used in our analyses.

Phase 1: Procedure and Clustering Analysis of Questionnaire Data—

Participants completed the questionnaire measures outlined above online. Incomplete data sets were excluded, and scores on each questionnaire scale were zero-meaned. The data were then submitted to a hierarchical nearest neighbor clustering analysis (using Ward's linkage criterion; Ward, 1963). Hierarchical clustering calculates pairwise distance values between each combination of scales based on correlation coefficients and uses these to create a hierarchical cluster tree, with branches representing different dimensions and subdimensions of affect (Figure 1). Using different cutoffs, it is possible to focus on alternate levels of analysis (e.g., depression versus anxiety-related affect or the next level down within the anxiety "branch"). Previous studies have performed clustering and correlational analyses both at the level of individual items (Bieling et al., 1998) and at the level of questionnaire scales (Watson et al., 1995). The item-level approach has been particularly valuable in measure development and validation. In this study, our aim was to extend beyond previous imaging studies that have typically focused on a single existing questionnaire scale, while providing an approach that could easily be adopted by the psychiatric neuroimaging community and that would also facilitate cross-study comparability. As such, we chose to perform our clustering at the level of existing validated (sub)scales.

Phase 2: Procedure and Data Acquisition for the Resting State fMRI Study—

After arriving at the University of California-Berkeley Brain Imaging Center, participants completed the nine standardized negative affect questionnaires, as described above. After this, they took part in a motion training session initially devised for children being scanned at the Brain Imaging Center facility. This involved lying inside our mock scanner (decommissioned 4T), watching a video. A sensor attached to the participant's forehead allowed a receiver attached to the headcoil to constantly record head motion. This in turn signaled the video to cut out if motion greater than a given threshold occurred. The threshold was incrementally lowered using cutoffs from 4 mm down to 0.5 mm. As such, participants were trained to become familiar with and avoid small head movements. After motion training, participants were accompanied to the 3T MRI suite where the scan session was

conducted using a Tim Trio 3T MR system with 12-channel head coil. Structural images were acquired using a T1-weighted 3-D MPRAGE sequence with whole brain coverage (repetition time = 2300 msec, echo time = 2.98 msec, flip angle = 9°, slice thickness = 1 mm). During the two 6-min resting state scans, participants were asked to lie still and rest, eyes open, maintaining fixation on a central cross. BOLD images were acquired with echo-planar T2* weighted (EPI) imaging (36 slices, repetition time = 2210 msec, slice thickness = 3 mm, in-plane resolution = 3.5×3.5 mm, field of view = 64×64 matrix, echo time = 30 msec).

fMRI Preprocessing

Preprocessing was conducted using FSL (FMRIB Software Library, www.fmrib.ox.ac.uk/fsl). Motion correction was conducted using FMRIB's Linear Image Registration Tool (MCFLIRT; Jenkinson, Bannister, Brady, & Smith, 2002; Jenkinson & Smith, 2001). B0 unwarping using acquired field maps was performed using FMRIB's Utility for Geometrically Unwarping EPIs (FUGUE; Cusack, Brett, & Osswald, 2003; Jezzard & Balaban, 1995). Slice timing correction, spatial smoothing with a Gaussian kernel of 5 mm FWHM, and high-pass temporal filtering (cut-off full-width 100 sec) to remove low-frequency drift were applied. EPI data were registered to the individual's skull-stripped structural (Smith, 2002) using linear affine registration (FLIRT; Jenkinson et al., 2002; Jenkinson & Smith, 2001). Structural to standard space registration was conducted using both linear and nonlinear registration (FNIRT; Andersson, Jenkinson, & Smith, 2007a, 2007b).

To minimize influences of scanner-related and physiological noise, single-subject ICA was performed using FSL's MELODIC (Multivariate Exploratory Linear Optimized Decomposition into Independent Components; Beckmann & Smith, 2004). Components related to noise were identified by eye and verified using an automatic classifier algorithm (fsl.fmrib.ox.ac.uk/fsl/fslwiki/FIX) before removal. Components were classified as noise when either (i) the component time series revealed large individual spikes, (ii) the component only contained power in high frequencies (i.e., above 0.1 Hz) as identified in the frequency spectrum, or (iii) the component map showed characteristic "ringing" around the edge of the brain indicative of movement (Kelly et al., 2010). Additional denoising was achieved by removing variance associated with outside brain, white matter, and movement parameter time series.

In the light of recent work (Power, Barnes, Snyder, Schlaggar, & Petersen, 2012; Van Dijk, Sabuncu, & Buckner, 2012), we conducted additional checks for the influence of potential remaining motion-related artifacts on our findings. Quantitative comparison of approaches for reducing movement-related noise revealed that including either ICA cleanup or scrubbing (volume removal based on frame-wise displacement, cutoff 0.2 mm; Power et al., 2012) led to reduction of mean whole-brain intensity changes from one time point to the next (DVARS) over and above noise regression (ICA: average reduction = 18.3, $p < .01$; scrubbing: average reduction = 11.4, $p < .01$). The results of this comparison closely paralleled those using a 0.5-mm displacement cutoff as reported previously by Bijsterbosch, Smith, Forster, and Bishop (2013). An average of 19.5 frames (i.e., 13%) exceeded the FD > 0.2 threshold (range, 1–69). The number of frames removed did not correlate with any of the individual difference measures ($ps > .1$). Our choice to use noise regression plus ICA cleanup as the locally (FMRIB) in-house preferred approach was reinforced by the similar performance, across participants, of ICA and scrubbing for reducing DVARS, together with the potential superiority of ICA cleanup for reducing outliers on this measure (Bijsterbosch et al., 2013). However, for completeness, we repeated the analyses reported in the manuscript after a combination of both ICA and scrubbing. In all cases, noise regression was

also always conducted. Use of ICA clean up, scrubbing (at a 0.2-mm displacement cutoff) and noise regression led to a decrease in DVARS relative to ICA and noise regression (average reduction = 8.2, $p < .01$) and relative to scrubbing and noise regression (average reduction = 13.3, $p < .01$). Addition of scrubbing did not, however, impact the reported results, which remained significant using the thresholds previously adopted (for threshold details, see the section on "Hierarchical clustering analysis of resting state networks"). The results reported throughout the Results section are hence those following our locally preferred cleanup approach of ICA combined with noise regression.

Selection and Redefinition of ROIs

ROIs for cortical and subcortical regions previously implicated in emotion-related processing (amygdala, caudate, hippocampus, thalamus, cingulate, paracingulate, ventromedial pFC [VMPFC, medial frontal Harvard–Oxford template], insula, and precuneous) were taken from the Harvard–Oxford atlas. For ROIs difficult to define anatomically, functionally defined ROIs were derived from a second-level group analysis of task-related fMRI data obtained from the same participants. Bilateral ROIs for lateral OFC were obtained using a localizer requiring processing of emotionally provocative stimuli. Participants viewed negative, ambiguously valenced, and neutral images from the International Affective Picture System (Lang, Bradley, & Cuthbert, 2008) in two imaging runs (60 images per run). Each image was displayed for 1 sec, and the ISI was jittered using an exponential function (min = 3 sec, mean = 6 sec). The second-level group contrast between emotionally ambiguous and negative images was used to create ROIs for the left OFC (peak Montreal Neurological Institute [MNI] coordinate [−36 52 −8]) and the right OFC (peak MNI coordinate [40 56 −4]). Additional ROIs were functionally localized using an fMRI-optimized version of the sustained attention to response (SART) task. (Forster, Nunez-Elizalde, Castle, & Bishop, under review; Fassbender et al., 2004; Robertson, Manly, Andrade, Baddeley, & Yiend, 1997). Participants were presented with single digits in a randomized order and instructed to respond to every digit that appeared (SART go trials), with the exception of the digit "3" (SART no-go trials). Each stimulus was presented for 250 msec followed by mask presentation (750–1050 msec). SART task blocks were alternated with control blocks that used letter stimuli and contained only go trials. There were 30 SART and 30 control blocks in total. Each block comprised 28 trials, the SART blocks including three no-go trials. The second-level group activation map to SART no-go trials was used to define ROIs for the SMA (peak MNI coordinate [−6 0 58]), left anterior insula (peak MNI coordinate [−38 10 −2]), right anterior insula (peak MNI coordinate [30 12 14]), left intraparietal cortex (IPC; peak MNI coordinate [−58 −40 38]), and right IPC (peak MNI coordinate [54 −48 36]). The second-level group contrast for SART go trials minus control go trials was used to define the right dorsolateral pFC (DLPFC; peak MNI coordinate [40 20 34]), and the left DLPFC was defined by flipping this right DLPFC cluster.

Bilateral posterior insula ROIs were obtained by subtraction of the anterior insula ROIs from the Harvard–Oxford anatomical ROIs for the insula. The Harvard–Oxford ROIs for the anterior and posterior cingulate cortex (ACC and PCC) were also further subdivided into pregenual ACC, anterior midcingulate cortex (aMCC), posterior midcingulate cortex (pMCC), and PCC. The subdivisions were guided by previous work addressing this issue (Shackman et al., 2011). The boundary between pregenual ACC and the aMCC was placed at $y = 30$, the boundary between aMCC and pMCC was positioned at $y = 4.5$, and the boundary between pMCC and PCC was placed at $y = −22$. Lastly, the Harvard–Oxford ROI for the paracingulate cortex was subdivided into anterior, middle, and posterior sections. Here, the middle paracingulate cortex ROI was defined based on the "dorsomedial pFC" region described in Kim et al. (2011), extending 10 mm anterior and 10 mm posterior from the peak MNI coordinates reported [0 32 36]. ROI subdivisions are illustrated in Figure 2.

Subject-specific Redefinition of ROI Boundaries

Given that exact locations of functional brain regions vary from participant to participant, template or group-defined ROIs can never be optimal. As a step toward improving upon this, we conducted an additional processing stage of redefining ROI boundaries on a subject-by-subject basis. For each participant, median time courses were calculated from each of the original 29 predefined ROIs described above. These ROIs were then combined to form a single binary mask, which was dilated using a $3 \times 3 \times 3$ mm kernel, leading to a dilation of approximately one voxel in all directions. Time courses for all voxels within this dilated mask were extracted and correlated against the median time course of each of the original ROIs. (The median time series was chosen as the summary statistic as it is minimally biased by potential heterogeneity of the predefined ROIs). Each voxel was then reassigned to the ROI with which it showed the highest correlation coefficient in both resting state fMRI runs. Voxels were excluded from further analysis if the maximum correlation did not result in a consistent ROI allocation across both fMRI runs. The largest contiguous cluster of voxels reallocated to a given ROI (i.e., correlating higher with the median time series of that ROI than any other ROI, across both runs) was used as the redefined ROI for that participant. In this manner, we created redefined subject-specific ROIs for all participants (Figure 2B and D). Mean time series were extracted from these subject-specific redefined ROIs and were used for all further analyses.

Hierarchical Clustering Analysis of Resting State Networks

Hierarchical nearest neighbor clustering was performed on time courses extracted from the 29 ROIs (temporally concatenated across participants). We identified a level of the resulting hierarchical tree that distinguished networks of similar complexity and potential functional relevance (Figure 3). These networks were used to investigate resting state correlates of the emergent anxiety-related dimensions of negative affect. Between-ROI correlation matrices were calculated for each participant and z-transformed using Fisher's transform, with the sign removed, before calculating connectivity indices. These were entered as dependent variables into a series of regression analyses. The indices used comprised (i) mean within-network connectivity, (ii) mean node-to-network connectivity (a "node" corresponding to a single ROI), and (iii) mean between-network connectivity. Questionnaire scale summary scores (zero-meaned) were entered as predictor variables. By entering one or more summary scores, while partialling out the effects of others, it was possible to examine differences in brain connectivity uniquely associated with the anxiety-related dimensions of affect derived from Phase 1. Nonparametric permutation testing (using Randomise: fsl.fmrib.ox.ac.uk/fsl/fslwiki/Randomise) was used for all analyses, and cross-run test–retest replicability was established using a threshold of (i) $p < .025$ in Run 1 and $p < .05$ in Run 2 (or vice versa) or (ii) $p < .05$ in Run 1 and $p < .1$ in Run 2 (or vice versa). These thresholds were chosen to reflect a two-sided t test in Run 1, followed by a confirmatory one-sided t test in Run 2 (or vice versa). Nonparametric permutation testing permutes subject labels and creates a null distribution of the maximum voxel-wise test statistic across the results obtained for each permutation (Nichols & Holmes, 2002). All reported within-network results additionally passed family-wise error correction for multiple comparisons, across the six networks that were tested, in at least one of the two resting state runs (at $p < .05$).

Additional Node-to-Node Analyses of Amygdala Connectivity

In addition to these primary analyses, we additionally examined node-to-node connectivity between the amygdala and medial prefrontal ROIs. This was conducted to facilitate comparisons with previous seed-based analyses of amygdala connectivity and its modulation by trait anxiety (e.g., Kim et al., 2011). In addition to our VMPFC ROI, two dorsal medial prefrontal regions were examined. As detailed above, our middle paracingulate cortex ROI

equates most directly to the dorsomedial prefrontal cortical region reported by Kim and colleagues. The nearby aMCC region, at times referred to as dorsal ACC (Bush, 2010), has been suggested to have closely related functionality (Kim et al., 2011; Shackman et al., 2011). *z*-Transformed correlation coefficients between left and right amygdala, VMPFC, aMCC, and middle paracingulate cortex were regressed against trait anxiety and against the questionnaire summary scores (as described above).

RESULTS

Phase 1: Clustering Analysis of Questionnaire Data

Hierarchical clustering analysis of the questionnaire data revealed a top-level distinction between measures tapping anxiety and depression-related affect (Figure 1). Two sub-clusters were anxiety related: one cognitive (Neuroticism, Penn State Worry Questionnaire, and STAI trait anxiety) and one physiological (MASQ anxious arousal and Anxiety Sensitivity Index). In addition, two depression-related subclusters indexed negative mood (Beck Depression Inventory and Center for Epidemiologic Studies Depression Scale) and anhedonia (MASQ anhedonic depression and STAI trait depression).

Phase 2: Cross-subject Brain Network Clustering Analysis of fMRI Data

Hierarchical clustering of ROI time series revealed six small-scale networks (Figure 3). Bilateral anterior and posterior insula regions formed one network (insula network). VMPFC, anterior paracingulate, and pregenual and subgenual ACC formed a second network (medial prefrontal network). The third "amygdala–hippocampal" network comprised bilateral amygdala and hippocampus ROIs. Bilateral caudate, thalamus, and lateral OFC ROIs formed an "OFC–subcortical" network. A "frontoparietal–PCC–precuneous" network consisted of PCC, precuneous, and middle and posterior paracingulate cortices together with bilateral DLPFC and IPC. It is of note that a further level of subdivision splits this into two networks comprising executive regions (DLPFC, middle paracingulate cortex, and IPC) versus default mode regions (PCC and precuneous). Lastly, the "cingulate network" comprised SMA, aMCC, and pMCC.

Relating Resting State Connectivity to Anxiety-related Dimensions of Negative Affect

The primary aim of the current study was to identify changes in resting state connectivity unique to anxious affect. Hence, after establishing the dimensional structure of our measures of negative affect in Phase 1, followed by cross-subject identification of resting state networks in Phase 2, we turned to investigating whether resting state connectivity varied as a function of the emergent anxiety-related dimensions of negative affect. Regression analyses were conducted to examine how (i) within-network, (ii) node-to-network, and (iii) between-network patterns of functional connectivity varied as a function of anxiety-related affect while controlling for depression-related measures.

Our first analysis positively weighted all anxiety-related measures, while controlling for depression-related measures, and hence reflects the top-level division between anxious and depressed affect. Results revealed that elevated anxiety-related affect was linked to decreased within-network connectivity in the insula network (Figure 4). To further explore this, we conducted an analysis of node-to-network connectivity using all ROIs within the insula network as nodes of interest. This revealed that all insula regions showed reduced within-network connectivity as a function of anxiety-related affect (Figure 5). Additionally, connectivity between right posterior insula and the amygdala–hippocampal network was decreased in participants with elevated anxiety-related affect. The latter was confirmed by analysis of insula to amygdala–hippocampal between-network connectivity (mean connectivity over all nodes that make up one network with all nodes that make up the other;

$p < .05$ in Run 1 and $p < .1$ in Run 2). Breaking the insula network down into anterior and posterior subregions (i.e., one level further down in the hierarchical tree) revealed that the reduction in within-network insula connectivity was driven by reduced connectivity between anterior and posterior insula subregions (Run 1: $T = 3.44$, $p < .01$; Run 2: $T = 1.81$, $p = .05$, see Figure 6).

Cognitive versus Physiological Subdimensions of Anxiety

We next investigated the subdimensions of anxiety identified in Phase 1 (namely cognitive and physiological anxiety) again using regression analyses with zero-meaned questionnaire scores entered as between-participant regressors. Here, only summary scores belonging to the subdimension of interest were weighted positively, enabling us to examine changes in connectivity uniquely associated with a given subdimension of affect while accounting for variance explained by the other measures.

Physiological anxiety was characterized by reduced within-network and node-to-network insula connectivity (Figures 4 and 5). The latter revealed widespread reduced connectivity of insula nodes, both with other insula subregions and with medial frontal and OFC–subcortical networks (Figure 5). Results from a between-network analysis confirmed decreased connectivity between the insula network as a whole and the OFC–subcortical network ($p < .05$ in Run 1 and $p < .1$ in Run 2).

A second major finding was that within-network connectivity in the frontoparietal–PCC–precunous network was significantly decreased as a function of physiological anxiety and increased as a function of cognitive anxiety (Figure 4). Node-to-network results revealed that this reflected altered involvement of DLPFC, paracingulate, and PCC (Figure 5).

Additional Node-to-Node Analyses of Amygdala Connectivity

The aim of the current study was to perform a data-driven multivariate analysis to identify differences in brain connectivity linked to cognitive and physiological anxiety. As such, we did not focus specifically on amygdala connectivity. However, given the value of comparability across studies, we additionally directly examined node-to-node connectivity between amygdala ROIs and both ventromedial and dorsomedial (aMCC and middle paracingulate cortex) ROIs included in this study. We investigated the extent to which node-to-node connectivity was modulated by STAI anxiety and by our clustering-derived summary measures of anxious affect. STAI trait anxiety was positively associated with amygdala–aMCC connectivity ($p = .05$, uncorrected). A parallel result was obtained using the physiological subdimension of anxiety ($p = .03$ uncorrected). There was no significant relationship between any of our anxiety indices and amygdala–middle paracingulate connectivity ($p > .1$). STAI trait anxiety also showed a trend level negative association with amygdala–VMPFC connectivity ($p = .07$ uncorrected). Here, parallel findings were observed using the physiological subdimension of anxiety ($p = .02$ uncorrected). These results broadly replicate previous findings using the STAI trait subscale (Kim et al., 2011).

DISCUSSION

The aim of the current study was to identify alterations in resting state functional connectivity specific to individual differences in anxiety. We used a two-stage multivariate clustering approach to first identity subdimensions of anxiety-related affect and then, controlling for depressed affect, to examine how resting state connectivity varied as a function of these dimensions of anxious affect.

Our hierarchical clustering analysis of data from standardized self-report measures of negative affect revealed a high degree of correlation between zero-meaned scores on these measures, in line with there being a common element to vulnerability for negative affect. The first major "branch" separated measures tapping tendency to anxious versus depressed affect, in line with Clark and Watson's tripartite model (Clark & Watson, 1991). The "anxiety" branch further subdivided into measures tapping physiological versus cognitive anxiety. Following this hierarchical structure, we investigated differences in resting state brain function linked to general tendency to anxious affect (controlling for depressed affect). Additionally, the emergent subdimensions of cognitive versus physiological anxiety were used to identify patterns of resting brain activity uniquely linked to each of these subdimensions over and above the other.

Findings revealed that both anxious affect (controlling for depressed affect), in general, and physiological anxiety, in specific, were associated with reduced connectivity between bilateral anterior and posterior insula (Figure 4). Furthermore, reduced connectivity between the insula and amygdala–hippocampal networks was linked to anxious affect in general, whereas decreased connectivity between insula nodes and both medial prefrontal and OFC–subcortical networks was additionally associated with physiological anxiety (Figure 5). Meanwhile, the cognitive anxiety subdimension of negative affective style was linked to greater connectivity between frontal–parietal and default mode (posterior cingulate, precuneous) regions.

The finding of widespread reductions in insula connectivity linked to anxiety and, in particular, the physiological subdimension of anxiety is of interest given that the insula has been implicated in a range of cognitive, emotional, and homeostatic processes including salience detection, awareness of bodily state, response to pain, and risky decision-making (Andreescu et al., 2011; Levens & Phelps, 2010; Paulus & Stein, 2010; Xue, Lu, Levin, & Bechara, 2010; Craig, 2002, 2009; Wiech & Tracey, 2009). There have been a number of recent parcellation studies of insular subregions, using a combination of resting state functional connectivity, structural connectivity, and meta-analyses of task-based coactivation (Chang, Yarkoni, Khaw, & Sanfey, 2013; Cauda et al., 2012; Kelly et al., 2012; Deen, Pitskel, & Pelphrey, 2011). These studies have consistently differentiated posterior and anterior insula subregions, with further differentiation within anterior insula being suggested by some reports (Chang et al., 2013; Kelly et al., 2012; Deen et al., 2011). The findings from these studies indicate extensive connectivity between the anterior insula and "executive control" regions (both medial and lateral frontal and parietal cortex). Meanwhile, findings from both imaging and anatomical tracing studies converge to suggest that the posterior insula plays a central role in the integration of interoceptive input received via the thalamus (Craig, 2002).

A recent integrative network model of insula function proposed by Menon and Uddin (2010) postulates that the insula acts as a key hub region, facilitating the controlled processing by attentional and working memory networks of information pertaining to stimulus salience and internal state. As in the earlier work by Craig (2002), interoceptive information is thought to pass via the thalamus to the posterior insula and then on to the anterior insula. Hence, connectivity between insula subregions may be as important for regulation of internal state as connectivity between the insula and other networks.

Here, we report an association between anxious affect and reduced connectivity between anterior and posterior insula subregions as well as between insula nodes and other networks (the amygdala–hippocampal, medial pre-frontal and OFC–subcortical networks). This may reflect diminished ability of the insula to activate regulatory control processes in response to changes in internal state and/or external events. The particular link with physiological

anxiety is consistent with a major aspect of this dysregulation entailing inability to regulate internal affective state, in particular its physiological expression. Here, it is of interest that regions belonging to the medial frontal network are widely thought to play a key role in emotion regulation. Our findings potentially suggest that the insula may act as an important intermediary hub in this process and that its functionality, including connectivity between anterior and posterior subregions, as well as with other cortical and subcortical regions, may play a role in individual differences in emotion regulation abilities.

Our analyses also revealed that connectivity within a frontoparietal–PCC–precuneous network was a differential marker of cognitive versus physiological anxiety (Figures 4 and 5). This network combines areas that are traditionally assigned to the "default mode network" with frontal and parietal regions associated with the "executive control network." In healthy volunteers, these two commonly found resting state networks are often observed to be anticorrelated. (Fox et al., 2005; Greicius, Krasnow, Reiss, & Menon, 2003). While our cross-subject clustering results did show that this network subdivides down into these two smaller networks (Figure 3), they were not anti-correlated. However, such anticorrelations may result from preprocessing strategies such as global signal regression and band pass filtering (Fox, Zhang, Snyder, & Raichle, 2009; Murphy, Birn, Handwerker, Jones, & Bandettini, 2009), which were not adopted in the current study. Furthermore, the deliberate inclusion of high anxious participants in our current study might account for the cross-group clustering of these regions in line with reported coactivation of these regions during "mind wandering" and worry (Christoff, 2012; Christoff, Gordon, Smallwood, Smith, & Schooler, 2009). Indeed, our finding that connectivity between these regions varies positively as a function of cognitive anxiety is in line with the view that cognitive aspects of anxiety may be linked to increased preoccupation with negative self-referential thoughts. In contrast, the reduced connectivity of the frontoparietal–PCC–precunus network in physiological anxiety may reflect superfluous attention on current physiological state, as opposed to internally generated cognitions. These differential resting state correlates of specific underlying constructs of anxiety potentially throw light on why some individuals show anxiety symptomatology with a strong "physiological" flavor, whereas others show more worry-related symptomatology. This in turn might suggest differential treatment routes for these subgroups of individuals. In future larger-scale studies, we wish to explore whether the resting state patterns identified here are robust across different populations (as characterized by gender and ethnicity) and to establish if they are indeed of value in predicting response to treatment. It is also our hope that the results presented here will encourage other researchers (in particular those conducting large-scale studies that lead to freely available databases) to include a wide range of self-report measures to allow more extensive identification and investigation of subdimensions of negative affect.

In conclusion, using a two-stage multivariate analysis of resting state fMRI data, we have identified alterations in within- and between-network functional connectivity uniquely associated with anxious as opposed to depressed affect. Furthermore, we report patterns of altered resting state brain connectivity linked specifically with physiological versus cognitive subdimensions of anxious affect. Our findings indicate that connectivity within a frontoparietal–PCC–precunus network comprising both frontal–parietal and default mode regions is differentially increased in cognitive anxiety and decreased in physiological anxiety. In addition, our findings suggest that altered insula connectivity with multiple regions may be a critical hallmark of physiological anxiety. These results are in line with proposals that the insula functions to facilitate regulatory control of affective state, acting as a key junction between medial frontal and subcortical regions (Menon & Uddin, 2010). We additionally observed that altered connectivity between posterior and anterior insula characterized both anxiety in general and physiological anxiety in specific. This finding

raises the need, in future research, to establish whether the disrupted insula connectivity patterns observed here primarily arise from dysfunction of one or both of these subregions.

Acknowledgments

References

Adelstein JS, Shehzad Z, Mennes M, DeYoung CG, Zuo XN, Kelly C, et al. Personality is reflected in the brain's intrinsic functional architecture. PLoS ONE. 2011; 6:e27633. [PubMed: 22140453]

Andersson JLR, Jenkinson M, Smith S. Non-linear optimization. FMRIB technical report. 2007a; TR07 JA1

Andersson JLR, Jenkinson M, Smith S. Non-linear registration, aka spatial normalisation. FRMIB technical report. 2007b; TR07 JA2

Andreescu C, Gross JJ, Lenze E, Edelman KD, Snyder S, Tanase C, et al. Altered cerebral blood flow patterns associated with pathologic worry in the elderly. Depression and Anxiety. 2011; 28:202–209. [PubMed: 21394853]

Baur V, Hänggi J, Langer N, Lutz J. Resting-state functional and structural connectivity within an insula-amygdala route specifically index state and trait anxiety. Biological Psychiatry. 2012 10.1016/j. biopsych.2012.06.003.

Beck AT, Ward CH, Mendelson M, Mock J, Erbaugh J. An inventory for measuring depression. Archives of General Psychiatry. 1961; 4:561–571. [PubMed: 13688369]

Beckmann CF, Smith SM. Probabilistic independent component analysis for functional magnetic resonance imaging. IEEE Transactions on Medical Imaging. 2004; 23:137–152. [PubMed: 14964560]

Bieling PJ, Antony MM, Swinson RP. The State–Trait Anxiety Inventory, Trait version: Structure and content re-examined. Behaviour Research and Therapy. 1998; 36:777–788. [PubMed: 9682533]

Bijsterbosch, JD.; Smith, S.; Forster, S.; Bishop, S. Quantitative evaluation of motion artifact reduction techniques in resting state fMRI data. Paper presented at the Human Brain Mapping; Seattle. 2013.

Bush G. Attention-deficit/hyperactivity disorder and attention networks. Neuropsychopharmacology. 2010; 35:278–300. [PubMed: 19759528]

Cauda F, Costa T, Torta DM, Sacco K, D'Agata F, Duca S, et al. Meta-analytic clustering of the insular cortex: Characterizing the meta-analytic connectivity of the insula when involved in active tasks. Neuroimage. 2012; 62:343–355. [PubMed: 22521480]

Chambers JA, Power KG, Durham RC. The relationship between trait vulnerability and anxiety and depressive diagnoses at long-term follow-up of generalized anxiety disorder. Journal of Anxiety Disorders. 2004; 18:587–607. [PubMed: 15275941]

Chang LJ, Yarkoni T, Khaw MW, Sanfey AG. Decoding the role of the insula in human cognition: Functional parcellation and large-scale reverse inference. Cerebral Cortex. 2013; 23:739–749. [PubMed: 22437053]

Christoff K. Undirected thought: Neural determinants and correlates. Brain Research. 2012; 1428:51–59. [PubMed: 22071565]

Christoff K, Gordon AM, Smallwood J, Smith R, Schooler JW. Experience sampling during fMRI reveals default network and executive system contributions to mind wandering. Proceedings of the National Academy of Sciences. 2009; 106:8719–8724.

Clark LA, Watson D. Tripartite model of anxiety and depression: Psychometric evidence and taxonomic implications. Journal of Abnormal Psychology. 1991; 100:316–336. [PubMed: 1918611]

Cole DM, Smith SM, Beckmann CF. Advances and pitfalls in the analysis and interpretation of resting-state fMRI data. Frontiers in Systems Neuroscience. 2010; 4:8. [PubMed: 20407579]

Costa PT Jr, McCrae RR. Domains and facets: Hierarchical personality assessment using the revised NEO personality inventory. Journal of Personality Assessment. 1995; 64:21–50. [PubMed: 16367732]

Craig AD. How do you feel? Interoception: The sense of the physiological condition of the body. Nature Reviews Neuroscience. 2002; 3:655–666.

Craig AD. How do you feel—Now? The anterior insula and human awareness. Nature Reviews Neuroscience. 2009; 10:59–70.

Cusack R, Brett M, Osswald K. An evaluation of the use of magnetic field maps to undistort echo-planar images. Neuroimage. 2003; 18:127–142. [PubMed: 12507450]

Deen B, Pitskel NB, Pelphrey KA. Three systems of insular functional connectivity identified with cluster analysis. Cerebral Cortex. 2011; 21:1498–1506. [PubMed: 21097516]

Dennis EL, Gotlib IH, Thompson PM, Thomason ME. Anxiety modulates insula recruitment in resting-state functional magnetic resonance imaging in youth and adults. Brain Connectivity. 2011; 1:245–254. [PubMed: 22433052]

Etkin A, Prater KE, Schatzberg AF, Menon V, Greicius MD. Disrupted amygdalar subregion functional connectivity and evidence of a compensatory network in generalized anxiety disorder. Archives of General Psychiatry. 2009; 66:1361–1372. [PubMed: 19996041]

Eysenck, H.; Eysenck, SBG. Eysenck Personality Questionnaire Manual. San Diego, CA: Educational and Industrial Testing Service; 1975.

Eysenck S, Eysenck H, Barrett P. A revised version of the Psychoticism Scale. Personality and Individual Differences. 1985; 6:21–29.

Fassbender C, Murphy K, Foxe JJ, Wylie GR, Javitt DC, Robertson IH, et al. A topography of executive functions and their interactions revealed by functional magnetic resonance imaging. Brain Research, Cognitive Brain Research. 2004; 20:132–143. [PubMed: 15183386]

Forster S, Nunez-Elizalde AO, Castle E, Bishop S. Unraveling the anxious mind: Anxiety, worry and frontal engagement in sustained attention versus off-task processing. under review.

Fox MD, Snyder AZ, Vincent JL, Corbetta M, Van Essen DC, Raichle ME. The human brain is intrinsically organized into dynamic, anticorrelated functional networks. Proceedings of the National Academy of Sciences, USA. 2005; 102:9673–9678.

Fox MD, Zhang D, Snyder AZ, Raichle ME. The global signal and observed anticorrelated resting state brain networks. Journal of Neurophysiology. 2009; 101:3270–3283. [PubMed: 19339462]

Greicius MD, Krasnow B, Reiss AL, Menon V. Functional connectivity in the resting brain: A network analysis of the default mode hypothesis. Proceedings of the National Academy of Sciences, USA. 2003; 100:253–258.

Hahn A, Stein P, Windischberger C, Weissenbacher A, Spindelegger C, Moser E, et al. Reduced resting-state functional connectivity between amygdala and orbitofrontal cortex in social anxiety disorder. Neuroimage. 2011; 56:881–889. [PubMed: 21356318]

Hettema JM, An SS, Bukszar J, van den Oord EJ, Neale MC, Kendler KS, et al. Catechol-O-methyltransferase contributes to genetic susceptibility shared among anxiety spectrum phenotypes. Biological Psychiatry. 2008; 64:302–310. [PubMed: 18436194]

Jenkinson M, Bannister P, Brady M, Smith S. Improved optimization for the robust and accurate linear registration and motion correction of brain images. Neuroimage. 2002; 17:825–841. [PubMed: 12377157]

Jenkinson M, Smith S. A global optimisation method for robust affine registration of brain images. Medical Image Analysis. 2001; 5:143–156. [PubMed: 11516708]

Jezzard P, Balaban RS. Correction for geometric distortion in echo planar images from B0 field variations. Magnetic Resonance in Medicine. 1995; 34:65–73. [PubMed: 7674900]

Kelly C, Toro R, Di Martino A, Cox CL, Bellec P, Castellanos FX, et al. A convergent functional architecture of the insula emerges across imaging modalities. Neuroimage. 2012; 61:1129–1142. [PubMed: 22440648]

Kelly RE Jr, Alexopoulos GS, Wang Z, Gunning FM, Murphy CF, Morimoto SS, et al. Visual inspection of independent components: Defining a procedure for artifact removal from fMRI data. Journal of Neuroscience Methods. 2010; 189:233–245. [PubMed: 20381530]

Kendler KS, Gardner CO, Gatz M, Pedersen NL. The sources of co-morbidity between major depression and generalized anxiety disorder in a Swedish national twin sample. Psychological Medicine. 2007; 37:453–462. [PubMed: 17121688]

Kim MJ, Gee DG, Loucks RA, Davis FC, Whalen PJ. Anxiety dissociates dorsal and ventral medial prefrontal cortex functional connectivity with the amygdala at rest. Cerebral Cortex. 2011; 21:1667–1673. [PubMed: 21127016]

Lang PJ, Bradley MM, Cuthbert BN. International affective picture system (IAPS): Affective ratings of pictures and instruction manual. 2008

Levens SM, Phelps EA. Insula and orbital frontal cortex activity underlying emotion interference resolution in working memory. Journal of Cognitive Neuroscience. 2010; 22:2790–2803. [PubMed: 20044897]

McIntosh AR, Bookstein FL, Haxby JV, Grady CL. Spatial pattern analysis of functional brain images using partial least squares. Neuroimage. 1996; 3:143–157. [PubMed: 9345485]

McIntosh AR, Chau WK, Protzner AB. Spatiotemporal analysis of event-related fMRI data using partial least squares. Neuroimage. 2004; 23:764–775. [PubMed: 15488426]

Menon V, Uddin L. Saliency, switching, attention and control: A network model of insula function. Brain Structure and Function. 2010; 214:655–667. [PubMed: 20512370]

Meyer TJ, Miller ML, Metzger RL, Borkovec TD. Development and validation of the Penn State Worry Questionnaire. Behaviour Research and Therapy. 1990; 28:487–495. [PubMed: 2076086]

Murphy K, Birn RM, Handwerker DA, Jones TB, Bandettini PA. The impact of global signal regression on resting state correlations: Are anti-correlated networks introduced? Neuroimage. 2009; 44:893–905. [PubMed: 18976716]

Nichols TE, Holmes AP. Nonparametric permutation tests for functional neuroimaging: A primer with examples. Human Brain Mapping. 2002; 15:1–25. [PubMed: 11747097]

Pannekoek JN, Veer IM, van Tol M-J, van der Werff SJA, Demenescu LR, Aleman A, et al. Resting-state functional connectivity abnormalities in limbic and salience networks in social anxiety disorder without comorbidity. European Neuropsychopharmacology. 201210.1016/j.euroneuro. 2012.04.018

Paulus MP, Stein MB. Interoception in anxiety and depression. Brain Structure & Function. 2010; 214:451–463. [PubMed: 20490545]

Plehn K, Peterson RA. Anxiety sensitivity as a predictor of the development of panic symptoms, panic attacks, and panic disorder: A prospective study. Journal of Anxiety Disorders. 2002; 16:455–474. [PubMed: 12213039]

Power JD, Barnes KA, Snyder AZ, Schlaggar BL, Petersen SE. Spurious but systematic correlations in functional connectivity MRI networks arise from subject motion. Neuroimage. 2012; 59:2142–2154. [PubMed: 22019881]

Radloff LS. The CES-D Scale: A self-report depression scale for research in the general population. Applied Psychological Measurement. 1977; 1:385–401.

Reiss S, Peterson RA, Gursky DM, McNally RJ. Anxiety sensitivity, anxiety frequency and the prediction of fearfulness. Behaviour Research and Therapy. 1986; 24:1–8. [PubMed: 3947307]

Robertson IH, Manly T, Andrade J, Baddeley BT, Yiend J. "Oops!": Performance correlates of everyday attentional failures in traumatic brain injured and normal subjects. Neuropsychologia. 1997; 35:747–758. [PubMed: 9204482]

Seeley WW, Menon V, Schatzberg AF, Keller J, Glover GH, Kenna H, et al. Dissociable intrinsic connectivity networks for salience processing and executive control. The Journal of Neuroscience. 2007; 27:2349–2356. [PubMed: 17329432]

Shackman AJ, Salomons TV, Slagter HA, Fox AS, Winter JJ, Davidson RJ. The integration of negative affect, pain and cognitive control in the cingulate cortex. Nature Reviews Neuroscience. 2011; 12:154–167.

Smith SM. Fast robust automated brain extraction. Human Brain Mapping. 2002; 17:143–155. [PubMed: 12391568]

Spielberger, CD. Manual for the State–Trait Anxiety Inventory. Palo Alto, CA: Consulting Psychologists Press; 1983.

Van Dijk KRA, Sabuncu MR, Buckner RL. The influence of head motion on intrinsic functional connectivity MRI. Neuroimage. 2012; 59:431–438. [PubMed: 21810475]

Ward JH. Hierarchical grouping to optimize an objective function. Journal of the American Statistical Association. 1963; 58:236–244.

Watson, D.; Clark, LA. The Mood and Anxiety Symptom Questionnaire. Iowa City, IA: Department of Psychology, University of Iowa; 1991.

Watson D, Weber K, Assenheimer JS, Clark LA, Strauss ME, McCormick RA. Testing a tripartite model: I. Evaluating the convergent and discriminant validity of anxiety and depression symptom scales. Journal of Abnormal Psychology. 1995; 104:3–14. [PubMed: 7897050]

Wiech K, Tracey I. The influence of negative emotions on pain: Behavioral effects and neural mechanisms. Neuroimage. 2009; 47:987–994. [PubMed: 19481610]

Xue G, Lu Z, Levin IP, Bechara A. The impact of prior risk experiences on subsequent risky decision-making: The role of the insula. Neuroimage. 2010; 50:709–716. [PubMed: 20045470]
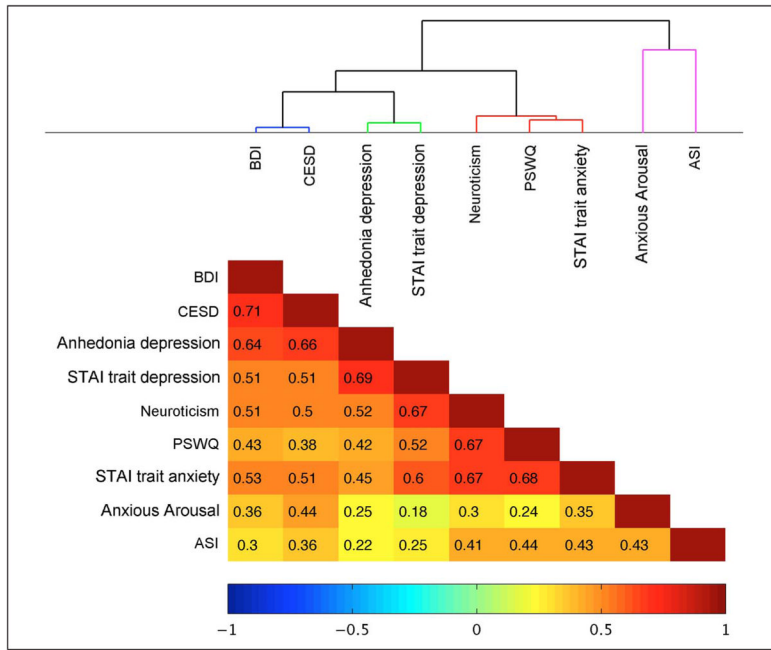
Figure 1.
Results from a hierarchical clustering analysis performed on questionnaire data obtained online (n = 327) using nine measures obtained from standardized self-report questionnaires assessing aspects of negative affective style. The cluster tree (top) reveals four main clusters of negative affect. Colors and numeric values in the correlation matrix (bottom) indicate correlation strength (Pearson's r). BDI = Beck Depression Inventory; CESD = Center for Epidemiologic Studies Depression Scale. Anhedonia Depression and Anxious Arousal subscales are from the MASQ. STAI trait depression and STAI trait anxiety together comprise the Spielberger STAI trait subscale (Spielberger, 1983). The Neuroticism Scale is from the Eysenck Personality Questionnaire. PSWQ = Penn State Worry Questionnaire. ASI = Anxiety Sensitivity Index.
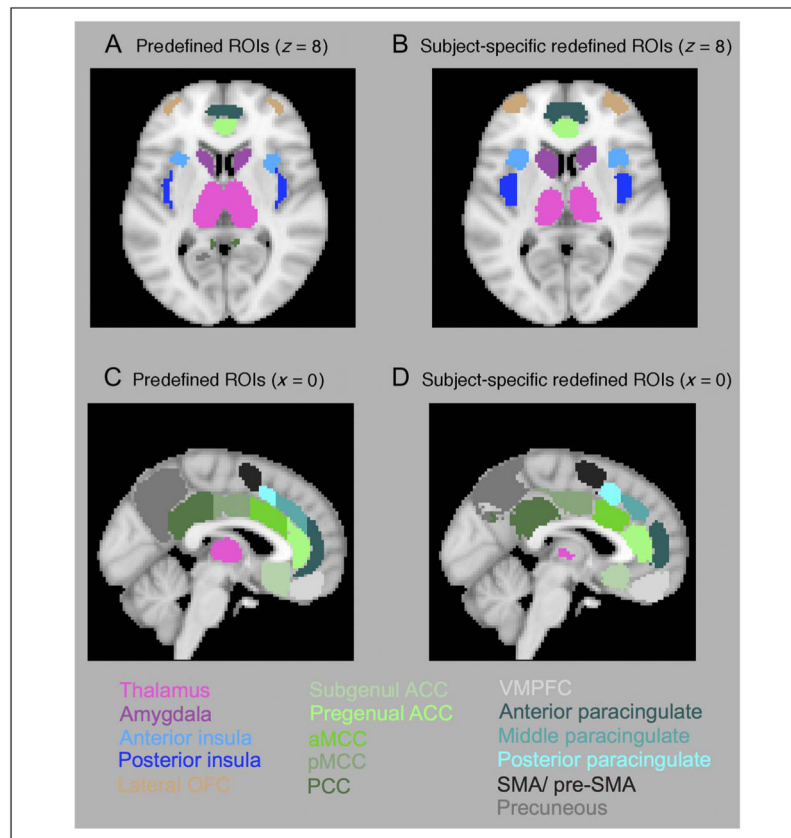
Figure 2.
Illustration of predefined ROIs (left) and the voxel-wise mode of subject-specific redefined ROIs (right). (A, B) Illustration of the redefinition of boundaries between the anterior and posterior insula on a transverse slice ($z = 8$). (C, D) Illustration of the redefinition of boundaries in the cingulate cortex on a sagittal slice ($x = 0$). DMPFC = dorsomedial pFC.
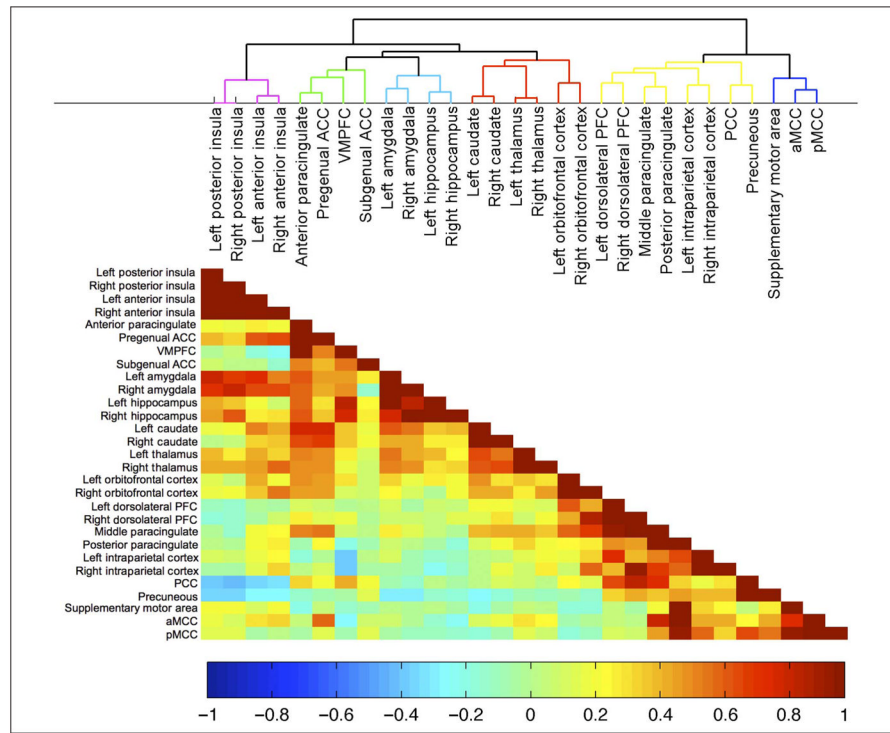
Figure 3.
Mean resting state connectivity networks as measured by hierarchical clustering analysis of correlation between resting state BOLD time series derived from 29 subject-specific redefined ROIs (see also Figure 2). The cluster tree (top) shows that the 29 regions cluster into six subnetworks. Colors within the correlation matrix (bottom) indicate correlation strength.
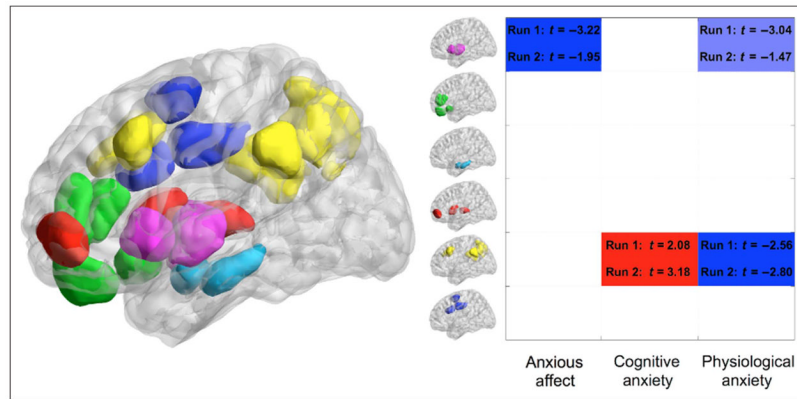
Figure 4.
Differences in within-network connectivity associated with negative affective style. The image on the left shows all redefined ROIs on a three-dimensional image of the brain viewed from the left side (as visualized with the BrainNet Viewer; www/nitrc.org/projects/ bnv). ROI colors reflect network membership as indicated in Figure 3 (purple = insula, green = medial prefrontal, light sky blue = amygdala–hippocampal, red = OFC–subcortical, yellow = frontoparietal–PCC–precunous, blue = cingulate). The table on the right shows differences in within-network connectivity as a function of (i) anxious affect (controlling for depressed affect)—representing the top level of branching within the hierarchical cluster tree of negative affect, (ii) cognitive anxiety (one subdimension of anxious affect), and (iii) physiological anxiety (the other subdimension of anxious affect). Each row in the table represents a different brain network (color coding as in Figure 3). Cell color indicates direction and strength of differences in connectivity. Blue indicates a decrease in within-network connectivity, and red indicates an increase. Dark blue and red indicate connectivity differences that were significant at a threshold of $p < .025$ in Run 1 and $p < .05$ in Run 2 (or vice versa). Light blue indicates connectivity decreases that were significant at $p < .05$ in Run 1 and $p < .1$ in Run 2 (or vice versa); t statistics for Runs 1 and 2 are provided.
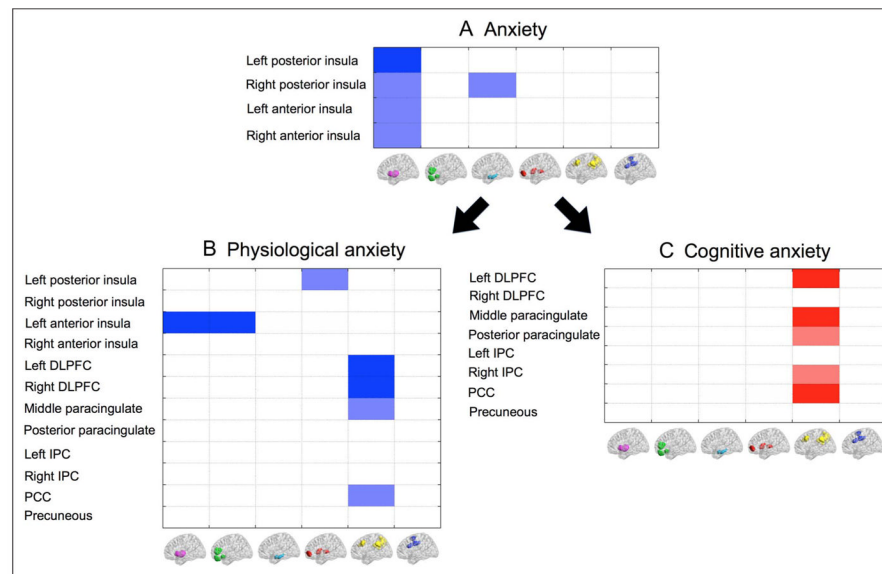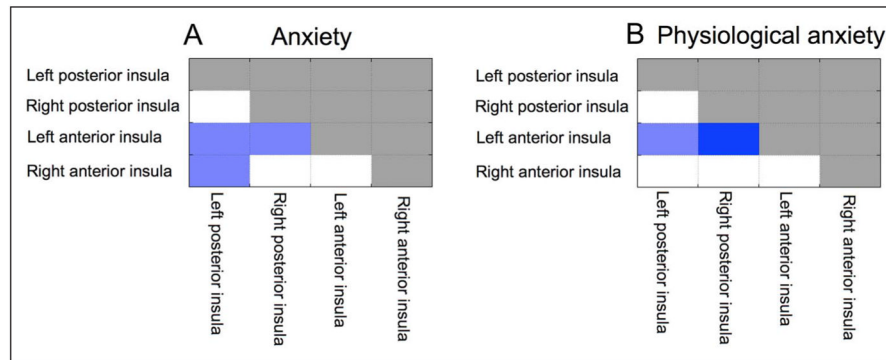
Figure 5.
Differences in node-to-network resting state connectivity associated with (A) anxious affect, (B) the physiological subdimension of anxiety, and (C) the cognitive subdimension of anxiety. Each table row represents a different brain network (color coding as in Figures 3 and 4). Cell color indicates direction and strength of differences in connectivity. Blue indicates a decrease in node-to-network connectivity, and red indicates an increase. Dark blue and red indicate connectivity differences that were significant at a threshold of $p < .025$ in Run 1 and $p < .05$ in Run 2 (or vice versa). Light blue and light red indicate connectivity decreases that were significant at $p < .05$ in Run 1 and $p < .1$ in Run 2 (or vice versa).

Figure 6.
Node-to-node insula connectivity for anxious affect in general (A) and for physiological anxiety in specific (B). Reduced connectivity between left posterior insula and bilateral anterior insula was associated with anxious affect in general and with physiological anxiety in specific. Dark blue indicates connectivity decreases that were significant at a threshold of $p < .025$ in Run 1 and $p < .05$ in Run 2 (or vice versa). Light blue indicates connectivity decreases that were significant at $p < .05$ in Run 1 and $p < .1$ in Run 2 (or vice versa).